Received: 3 February 2018 | Revised: 28 June 2018 | Accepted: 1 August 2018

DOI: 10.4218/etrij.2018-0027

ORIGINAL ARTICLE

WILEY ETRI Journal

Zero forcing based sphere decoder for generalized spatial modulation systems

Sara Jafarpoor[1] | **Majid Fouladian**[1] | **Mohammad Neinavaie**[2]

[1]Department of Electrical Engineering, College of Technical and Engineering, Saveh Branch, Islamic Azad University, Saveh, Iran.

[2]Department of Electrical Engineering, College of Technical and Engineering, Tehran Branch, Islamic Azad University, Tehran, Iran.

Correspondence
Majid Fouladian, Department of Electrical Engineering, College of Technical and Engineering, Saveh Branch, Islamic Azad University, Saveh, Iran.
Email: majidfouldadian@gmail.com

To reduce the number of radio frequency (RF) chains in multiple input multiple output (MIMO) systems, generalized spatial modulation (GSM) techniques have been proposed in the literature. In this paper, we propose a zero-forcing (ZF)-based detector, which performs an initial pruning of the search tree that will be considered as the initial condition in a sphere decoding (SD) algorithm. The proposed method significantly reduces the computational complexity of GSM systems while achieving a near maximum likelihood (ML) performance. We analyze the performance of the proposed method and provide an analytic performance difference between the proposed method and the ML detector. Simulation results show that the performance of the proposed method is very close to that of the ML detector, while achieving a significant computational complexity reduction in comparison with the conventional SD method, in terms of the number of visited nodes. We also present some simulations to assess the accuracy of our theoretical results.

KEYWORDS
diversity, generalized spatial modulation, multiple input multiple output, sphere decoding, zero-forcing

1 | INTRODUCTION

Multipath propagation leads to a signal fading effect, which can be mitigated using diversity in wireless systems [1]. Diversity is achieved by sending signals carrying the same information via independently faded paths. Multiple input multiple output (MIMO) systems provide space diversity, which potentially increases the available degree of freedom. Among the different transmitting techniques in MIMO systems, the Vertical Bell Lab Layered Space-Time (V-BLAST) method is capable of achieving receive diversity and exploiting the maximum degree of freedom in a wireless channel [2–5]. However, some of the challenges in MIMO systems include designing a diversity and multiplexing achieving technique, the cost of radio frequency (RF) chains, and the complexity of joint detection at the receiver.

In order to overcome the challenge of the cost of multiple RF chains, spatial modulation (SM) techniques are introduced, in which the transmit antennas are selected according to the data symbols. The SM method provides the benefit of multiple transmit antennas and a lower number of RF chains. In the SM method, only one antenna is active for transmitting the data, and the input data bits are split into two groups [6]. One of the groups is used to select the active antenna and the other one determines the transmitting symbol. In this method, besides modulating the data with a typical modulation scheme, the index of the active antenna has information in its own right and can be considered as a new spatial dimension for the modulation. This characteristic of SM systems reduces the implementation complexity cost due to the lower number of RF chains [6].

However, SM has certain limitations: (a) The number of transmit antennas has to be a power of two, which limits the designing flexibility. (b) The SM algorithm fails to exploit the available degrees of freedom since it deploys only one antenna to transmit data. In the GSM technique,

there are multiple transmit antennas, not all of which are active [7,8]. The active transmit antennas may send the same or different data symbols in order to achieve the available diversity or degrees of freedom, respectively. The GSM method can be considered as a combination of spatial modulation and spatial multiplexing techniques. This leads to a higher or equal spectral efficiency with lower transmit antennas in comparison with the SM method [8].

Generally, in MIMO communication systems, the maximum likelihood (ML) detector achieves the maximum receive diversity. However, the ML method is not practical due to the very high computational complexity arising from the massive joint search [9,10]. The computational complexity of the ML method increases exponentially with the number of transmit antennas. In the GSM method, the indices of the active antennas and data symbols have to be searched jointly. Therefore, the computational complexity of the receiver is still very high for the ML method. Numerous detection methods have been provided in literature. Some of these methods reduce the detection method to a tree search using the QR decomposition of the channel matrix [10]. From the perspective of tree search, the sphere decoding (SD) algorithm is an efficient solution for the ML search [9,10]. However, the SD and ML methods still suffer from an exponential computational complexity [10]. Several methods for reducing the computational complexity of the SD method have been presented in literature [11–16].

On the other hand, linear detection methods such as zero forcing (ZF) and minimum mean squared error (MMSE) benefit from a polynomial computational complexity [2]. However, linear detection methods suffer from poor performance and do not achieve the maximum available diversity [17]. In order to improve the performance of linear equalizers, the Lattice Reduction (LR) method is employed [18,19]. This method achieves the maximum receive diversity with a relatively lower performance in comparison with the ML method.

Several previous studies have demonstrated the feasibility of GSM and have proposed efficient detection methods. Renzo and others extensively studied SM, which can be regarded as GSM with a single active antenna [20,21]. Lee and others presented an efficient circuit-level implementation of a symbol detector for SM-MIMO systems [22]. Xiao and others proposed the ordered block (OB) minimum mean squared error (MMSE), where the transmit antenna combinations are sorted first and the symbol vector is estimated in sequence for each transmit antenna combination [23]. Chen and others employed a new criterion for sorting the transmit antenna combinations to reduce the complexity of the ordered block minimum mean squared error (OB-MMSE) [24]. Sphere decoding methods specialized for the SM-MIMO systems have been studied [25–27]. Cal-Braz and others showed how the conventional sphere decoding can be applied to GSM-MIMO detection, and evaluated the complexity of this method [28].

In this paper, we present a GSM MIMO detection method that achieves a near ML performance with a significantly low computational complexity. The contributions of this paper are summarized as follows:

- This paper generalizes the zero-forcing algorithm for a GSM MIMO system, which performs an initial pruning of the search tree. The SD algorithm searches the lattice points corresponding to a reduced search space. The reduction of the sphere-decoding step is due to the generalized ZF and the nature of GSM and inactive antennas.
- The proposed method is assessed analytically, and the performance is analyzed in terms of error probability. An analytical performance gap is derived in terms of a predetermined threshold, which gives the system designer a certain degree of freedom for the trade-off between complexity and performance, analytically.

The rest of this paper is organized as follows. Section 2 describes the system model. The search space reduction using the proposed zero-forcing method is presented in Section 3, and the proposed GSM detection algorithm is presented in Section 4. The performance is analyzed in Section 5. The simulation results are presented in Section 6 to assess the validity of the theoretical results. Finally, Section 7 concludes the paper.

2 | SYSTEM MODEL

Consider a multiple-antenna system with N_t transmit antennas and N_r receiver antennas, as shown in Figure 1. Let $\mathbf{H}$ denote the $N_r \times N_t$ MIMO channel matrix, and let M denote the number of the active transmit antennas, where $M < N_t$. The number of inactive antennas is denoted by $N_d = N_t - M$. In this setting, we can have $\binom{N_t}{M}$ possible combinations. In addition, let L be the BPSK size and K be the number of the antenna subsets used. To be more precise, $K = \left\lfloor \binom{N_t}{M} \right\rfloor_{2^P}$, where $\lfloor \rfloor_{2^P}$ is rounded down to the closest smaller power of two integers.

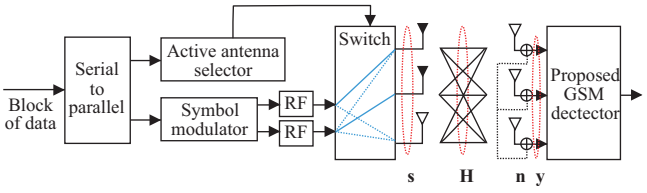

FIGURE 1 3 × 3 BPSK GSM MIMO system with two active antennas

At the transmitter, a block of independent information bits is first fed into a GSM mapper. In each block, the first $M\text{Log}_2(L)$ bits are mapped into a symbol vector denoted by $\mathbf{s} = [s_1, s_2, \ldots, s_M]^{\mathrm{T}}$, where $(.)^{\mathrm{T}}$ represents the transpose operation. Then, the spatial modulator uses the remaining $\text{Log}_2(K)$ bits to select the active transmit antennas, where $K \le \binom{N_t}{M}$. Let $\mathbf{H}_k$ denote the $N_r \times M$ MIMO channel submatrix corresponding to the active transmit antennas, where $k \in \{1, 2, \ldots, K\}$.

We assume that the elements of $\mathbf{H}_k$, that is, $[\mathbf{H}_k]_{ij}$, are identically and independently distributed (i.i.d.) complex Gaussian random variables with zero mean and unit variance. We also assume that $\mathbf{s}$ and $\mathbf{H}_k$ are generated independently. The received symbol vector can be expressed as:

$$\mathbf{y} = \mathbf{H}_k\mathbf{s} + \mathbf{n}, \tag{1}$$

where $\mathbf{n}$ is the white Gaussian noise vector with $E[\mathbf{n}\mathbf{n}^H] = \sigma^2\mathbf{I}$. The probability density function (PDF) of $\mathbf{y}$ conditioned on $\mathbf{H}_k$ and $\mathbf{s}$ can be written as:

$$f(\mathbf{y}|\mathbf{s}, \mathbf{H}_k) = \frac{1}{\left(\sqrt{\pi\sigma^2}\right)^{N_r}} \exp\left(-\|\mathbf{y} - \mathbf{H}_k\mathbf{s}\|_2^2\right). \tag{2}$$

Considering the maximum entropy, we assume that the transmitted symbols are equally probable. The joint ML detector for the transmitted symbols and active antennas is:

$$\{\hat{k}, \hat{\mathbf{s}}\} = \arg_{\substack{m \in \{1,2,\ldots,K\} \\ s \in S^M}} \min \|\mathbf{y} - \mathbf{H}_m\mathbf{s}\|_2^2, \tag{3}$$

where S^M is the search space of the transmitted symbol vector. The order of the ML search is KL^M.

On the other hand, the ZF detector solves (3) by neglecting the limited integer constraint, that is, $\mathbf{s} \in S^M$, as:

$$\{\hat{k}, \hat{\mathbf{s}}\} = \arg_{\substack{m \in \{1,2,\ldots,K\} \\ s \in R^M}} \min \|\mathbf{y} - \mathbf{H}_m\mathbf{s}\|_2^2. \tag{4}$$

The ZF detector calculates $\tilde{y}_m = \mathbf{H}_m^{\dagger}\mathbf{y}$, where $\mathbf{H}_m^{\dagger} = \left(\mathbf{H}_m^H\mathbf{H}_m\right)^{-1}\mathbf{H}_m^H$ for all possible values of m, and hence finds the smallest distance. In order to avoid the complexity of calculating the matrix inversion K times K, we propose the following the GSM-ZF method.

The equalized vector $\tilde{\mathbf{y}}$ can be expressed as:

$$\tilde{\mathbf{y}} = \mathbf{H}^{\dagger}\mathbf{y} = \mathbf{s} + \tilde{\mathbf{n}}, \tag{5}$$

where $\tilde{\mathbf{n}} = \mathbf{H}^{\dagger}\mathbf{n}$. By following the same procedure as that for the ZF method, the elements of $\tilde{y}$ have to be projected on the constellation points. However, since some of the transmit antennas may be inactive, the zero point is added to the constellation set to represent the inactive antennas. For instance, in the binary modulation using the GSM-ZF method, this projection has to be performed on the set $\{-1, 1, 0\}$ [28]. A problem that arises here is that the GSM-ZF method may claim the number of inactive antennas more than their actual number. This problem is addressed in the method proposed in Section 3.

3 | SEARCH SPACE REDUCTION USING THE PROPOSED ZERO-FORCING METHOD

Our proposed detection method searches a pruned detection tree to find the shortest path that corresponds to the optimal estimate. The detection tree is pruned via the GSM-ZF step.

To solve the detection problem for the system model of the GSM-MIMO shown in Figure 1, we consider the inactive antennas as zero points in the constellation set, that is, $S = \{-1, 1, 0\}$. For instance, for three transmit antennas and two active antennas, the detection tree is as shown in Figure 2. Next, we propose a method to prune this tree search and an algorithm to perform the search on the pruned tree.

We consider a threshold to generalize the ZF method as:

$$\log\frac{f(\tilde{y}_k|s_1)}{f(\tilde{y}_k|s_2)} \gtrless \text{th}, \tag{6}$$

where $\tilde{y}_k = \mathbf{H}_k^{\dagger}\mathbf{y}$. The PDF of the equalized vector $\tilde{y}_k$, which is conditioned on the transmit symbol s_i and channel matrix $\mathbf{H}$, can be expressed as:

$$f(\tilde{y}_k|s_i) = \frac{1}{\sqrt{2\pi\sigma_k^2}} \exp\left(-\frac{(\tilde{y}_k - s_i)^2}{2\sigma_k^2}\right), \tag{7}$$

where $\sigma_k^2 = \sigma^2\left[\left(\mathbf{H}^H\mathbf{H}\right)^{-1}\right]_{kk}$, $s_1 \in S$, $s_2 \in S$ and th is a predetermined threshold. The correlation imposed by the ZF algorithm reduces the performance of the detector inherently. However, an ML search is performed on the unreliable symbols detected by the ZF algorithm in the search space, in order to decrease the performance loss caused by ZF decoupling.

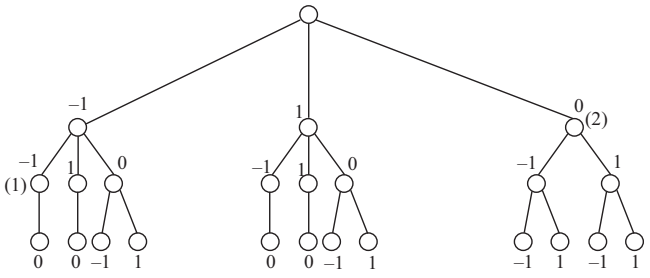

FIGURE 2 Detection tree for 3 × 3 BPSK GSM-MIMO system using two active antennas with added zero points

For instance, for $s_1 = 1$ and $s_2 = 0$, (6) yields:

$$\log\frac{f(\tilde{y}_k|s_1=1)}{(\tilde{y}_k|s_2=0)} = \log\frac{\frac{1}{\sqrt{2\pi\sigma_k^2}}\exp\left(-\frac{(\tilde{y}_k-1)^2}{2\sigma_k^2}\right)}{\frac{1}{\sqrt{2\pi\sigma_k^2}}\exp\left(-\frac{\tilde{y}_k{}^2}{2\sigma_k^2}\right)} \gtrless \text{th}, \quad (8)$$

which leads to $\tilde{y}_k \gtrless \sigma_k^2\text{th} + \frac{1}{2}$, where $\sigma_k^2\text{th} = \text{th}\left(\sigma^2\left[\left(\mathbf{H}^H\mathbf{H}\right)^{-1}\right]_{kk}\right)$ and $\sigma_k^2\text{th} = \text{th}_k$.

The ZF equalizer leads to a colored noise with the covariance matrix $\sigma^2(\mathbf{H}^H\mathbf{H})^{-1}$. It can be seen that the threshold relies on the covariance matrix of the colored noise and the SNR. The covariance matrix of the colored noise follows a Wishart distribution [17]. It should be noted that at high SNR, th_k tends to zero, which means that the algorithm relies on the ZF detector symbols at high SNR regime.

Similarly, we do the same calculations for the remaining collection points, which results in the following decision regions:

1. "Zero Region (ZR)": GSM inactive antenna region: $|\tilde{y}_k| < \frac{1}{2} - \text{th}_k$.

If the kth element of the equalized vector lies in this region, the kth antenna is considered to be inactive.

2. "One Region (R1)": GSM active antenna corresponding to symbol one: $\tilde{y}_k > \frac{1}{2} + \text{th}_k$.

If the kth element of the equalized vector lies in this region, the transmit symbol is considered to be one.

3. "Negative One Region (R-1)": GSM active antenna: $\tilde{y}_k < \frac{-1}{2} - \text{th}_k$.

If the kth element equalized vector lies in this region, the transmit symbol is considered to be negative one.

4. "Uncertainty One Region (U1)": the region where we should be doubtful about the ZF detector: $\frac{1}{2} - \text{th}_k < \tilde{y}_k < \frac{1}{2} + \text{th}_k$.

In this region, the ZF detector is undecided between zero and one.

5. "Uncertainty Negative One Region (U-1)": $\frac{-1}{2} - \text{th}_k < \tilde{y}_k < \frac{-1}{2} + \text{th}_k$.

In this region, the ZF detector is undecided between zero and negative one. These regions are summarized in Figure 3.

If the observation is in the uncertainty region, the SD algorithm performs search on the corresponding symbols.

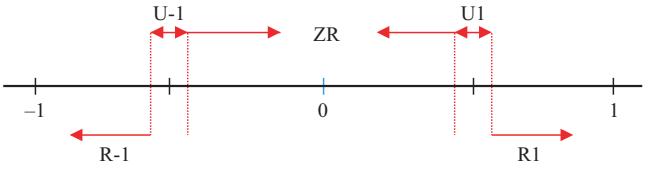

FIGURE 3 Zero, one, negative one, and uncertainty regions

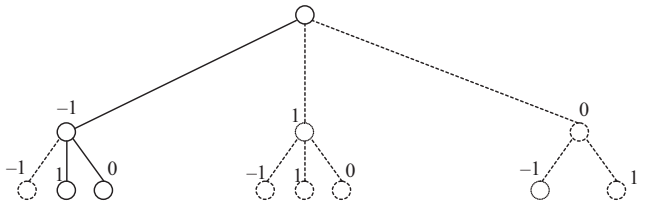

FIGURE 4 Pruned tree where $\tilde{y}_k < \frac{-1}{2} - \text{th}_k$ and $\frac{1}{2} - \text{th}_k < \tilde{y}_k < \frac{1}{2} + \text{th}_k$

For instance, if the observations of the first and the second antennas lie in R-1 and U1, respectively, the search tree is reduced to Figure 4.

This event can prune the search tree considerably, especially if it occurs at the primary nodes of the search tree. The set of selected symbols for the kth antenna is defined as D_k. Indeed, D_k is the kth search space and the total search space is defined as $D = \{D_1, D_2, \ldots, D_{N_t}\}$. For instance, in Figure 4, $D_1 = \{-1\}$ and $D_2 = \{1, 0\}$.

It should be noted that the number of antennas that the ZF detector detects in the inactive regions may be greater than the actual number of inactive antennas (N_d). In this case, we sort $\tilde{y}_k$ and choose N_d smallest antennas to be inactive, where $1 < N_\text{d} < N_\text{t}$ and the rest of the symbols are considered to be in the U1 or U-1 regions. We denote this event by $\mathcal{E}_1$ If the number of zeroes that the ZF-based algorithm declares is less than N_d, among the approved symbols, the ones whose observations are closer to zero are declared zero systematically. This event is also denoted by $\mathcal{E}_2$.

4 | PROPOSED GSM DETECTION ALGORITHM

In this section, we present the proposed method in more detail. This method generalizes the ZF detector by combining it with the generalized SD method for GSM-MIMO systems. By comparing the equalized observation with a threshold, we reduce the search space and the search candidates to create a subsearch space.

Next, the generalized SD algorithm is applied to perform the search in the provided space. Generally, the SD first selects a parameter R called the sphere radius. It then traverses the entire tree (say from left to right). However, once

it encounters a node with a cumulative metric larger than R, it does not follow down that branch. Hence, SD enumerates all the leaf nodes that lie inside the sphere $\|\mathbf{y} - \mathbf{Hs}\|^2 \leq R$. This also explains the name of the algorithm [29].

To make the problem tangible, we start with an example of a simple (not GSM) MIMO system. For instance, consider the case in which BPSK modulation is used with $N_t = 3$ and $N_r = 3$ (see Figure 5).

The lattice points (search candidates) for the SD algorithm can be seen in Figure 6. Each lattice point in Figure 6 is a branch on the search tree. For example, point (a) indicates the branch specified in Figure 5. In the SD algorithm, all the branches (candidate points) are searched inside a sphere with a radius R, and the minimum cost metric is considered as the transmitted symbol. For example, if point (a) has the minimum cost metric, this indicates that all three antennas have sent symbol 'one'.

However, in the proposed GSM-MIMO system, we encounter a different tree search. We consider the inactive antennas as a zero point in the constellation set, that is, $S = \{-1, 1, 0\}$. For instance, for three transmit antennas and BPSK modulation with one inactive antenna($N_d = 1$), the detection tree is as shown in Figure 2.

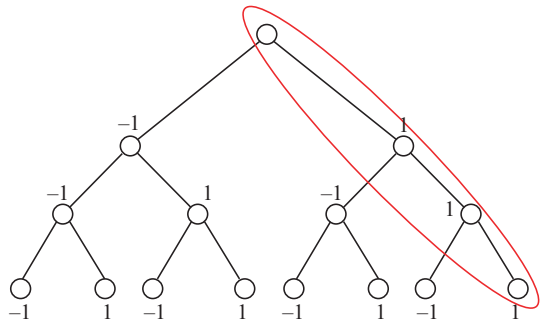

FIGURE 5 Detection tree for the 3 × 3BPSK MIMO system

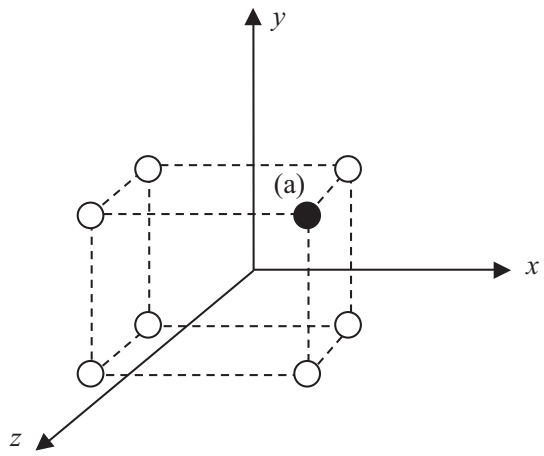

FIGURE 6 Lattice points for a traditional 3 × 3 BPSK MIMO system

The lattice points for this example are plotted in Figure 7. It should be noted that in a GSM system, the symmetrical structure of the lattices is changed due to the additional zeroes added to the constellation. For instance, in the three-dimensional example, some lattice points on the x-y, y-z, or x-z plane are added to the search space. In our proposed algorithm, the key point is the number of previous zeroes in each step. In each step, the number of zeroes in the previous step is counted; therefore, the following cases may occur. From the step where there are some remaining antennas and no antenna has been set to zero yet to the last step, we take into account only zeroes, and our search will not include the 1 and −1 points. For instance, in Figure 2, if we reach point (1), since we have met no zeroes yet, the next antenna has to be zero.

The next point is that in each step, if we have already counted N_d zeroes, from that step to the end, our search includes only 1 and −1 points, and the zero point will not be included. For instance, in Figure 2, if we reach point (2), since we have already counted one zero, (note that $N_d = 1$), we only consider –1 and 1 for the following steps.

Applying the ZF method, which equalizes the observation vector and compares them with some threshold, reduces the search candidates. Suppose that the filled points in Figure 7 are selected via the ZF algorithm. Therefore, the SD search is performed on these points and the point with the minimum cost metric is considered as the transmitted symbol. For example, if point (b) in Figure 7 has the minimum cost metric, the transmit symbols are considered to be 1, −1, and 0, respectively. The algorithm is summarized in Algorithm 1.

In our detection algorithm, we have used the Fincke-Pohst enumeration. However, some minor changes are applied to generalize the Fincke-Pohst algorithm for a GSM system. It should be noted that irrespective of the enumeration method used, the processing step reduces the number of search candidates in the SD algorithm, and thus, the total complexity is decreased.

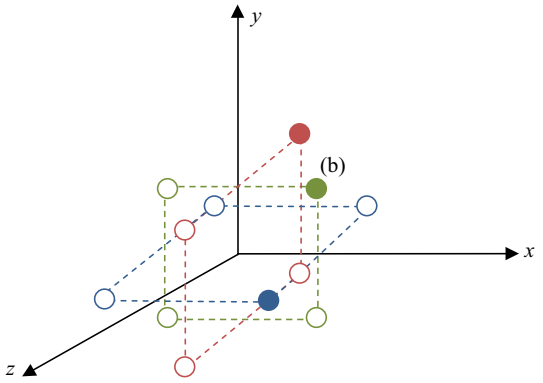

FIGURE 7 Lattice points for a 3 × 3 BPSK GSM-MIMO system with two active antennas

ALGORITHM 1 The proposed algorithm

Preprocessing

for k=1: M
$th_k=\sigma_k^2 th$
$\tilde{y} = H^{\dagger} y$
Equalization
Performing the region selection on $\tilde{y}_k$
eliminate the ambiguities ($\mathcal{E}_1, \mathcal{E}_2$)
Construct D_k
end

SD algorithm[1]

Input: y, R, set, t, distance
Output: $\hat{s}$ (detectedsymb)
set=D; k=size(s); $\hat{s}$ =zeros(k, 1);
find the QR decomposition of matrix H
temps=zeros(k, 1); FLAG=0; CNT=0; R=realmax;
$\tilde{y} = Q^T * y$;
GSM-SD($\tilde{y}$, R, set, k, 0);
if FLAG>0 r= $\hat{s}$;
else r=0
end

function GSM-SD(y, R, set, t, distance)
if we are visiting a leaf node (t=1)
find the number of zeroes;
if only one zero is remained
temps(1) = 0;
d = abs(y(1)-R(1,:)*temps)^2+distance;
if the metric d is smaller than the radius R
$\hat{s}$ =temps;
R=d;
FLAG=FLAG+1;
end
else
for i = 1:size of D_k(t)
temps(1) = set(t,i);
d = abs(y(1)-R(1,:)*temps)^2+distance;
if the metric d is smaller than the radius R
$\hat{s}$ =temps;
R=d;
FLAG=FLAG+1;
end
end
end
else
for i = 1:size of D_k(t)
if t=N_d and we have not had any zeroes yet
temps(t) =0;
end
temps(t) = set(t,i);
find the number of zeroes
if the number of zeroes is N_d
size of D_k(1:trans_antenna_no-1) =2;
end
d =abs(y(t)-R(t,t: end)*temps(t: end))^2+distance;
if the metric is smaller than R
GSM-SD(y, R, set, t-1, d);
end
end
end

*The SD algorithm is based on the Fincke-Pohst detection algorithm [29].

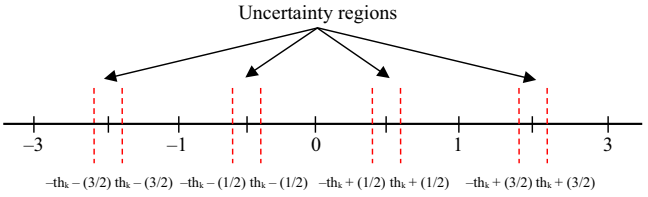

FIGURE 8 Decision regions for 4-PAM modulation

Generalization to Q^2-QAM:

The decision regions for the proposed method can be generalized for an arbitrary real lattice or Q-PAM modulation scheme. For instance, the regions for 4-PAM are demonstrated in Figure 8.

In addition, for a circularly symmetric complex Gaussian random vector, the system model in equation (1) can be rewritten as:

$$\begin{pmatrix} \mathrm{Re}(\mathbf{y}) \\ \mathrm{Im}(\mathbf{y}) \end{pmatrix} = \begin{pmatrix} \mathrm{Re}(\mathbf{H}_k) & -\mathrm{Im}(\mathbf{H}_k) \\ \mathrm{Im}(\mathbf{H}_k) & \mathrm{Re}(\mathbf{H}_k) \end{pmatrix} \begin{pmatrix} \mathrm{Re}(\mathbf{s}) \\ \mathrm{Im}(\mathbf{s}) \end{pmatrix} + \begin{pmatrix} \mathrm{Re}(\mathbf{n}) \\ \mathrm{Im}(\mathbf{n}) \end{pmatrix},$$

where Re(.) and Im(.) denote the real and modulation imaginary parts, respectively. Consequently, in Q^2-QAM, Re(s) and Im(s) can be assumed to be Q-PAM modulated signals. Using this complex to real conversion, we can generalize the decision regions in the preprocessing step to a Q^2-QAM modulation.

5 | PERFORMANCE ANALYSIS

In this section, we derive the upper bound of the error probability of the proposed algorithm. We first expand P_e as:

$$P_e = E_H\{E_s\{P_s(\hat{\mathbf{s}} \neq \mathbf{s}|\mathbf{H})\}\}, \tag{9}$$

where $P_s(\mathcal{E})$ is the probability that event $\mathcal{E}$ occurs, given that $\mathbf{s}$ is transmitted, ie $P(\mathcal{E}) = E_s\{P_s(\mathcal{E})\}$.

We make the expansion [16]:

$$\begin{aligned} P_s(\hat{\mathbf{s}} \neq \mathbf{s}|\mathbf{H}) &= P_s(\hat{\mathbf{s}} \neq \mathbf{s}|\mathbf{s} \in D, \mathbf{H}) \\ &\times P_s(\mathbf{s} \in D|\mathbf{H}) + P_s(\hat{\mathbf{s}} \neq \mathbf{s}|\mathbf{s} \notin D, \mathbf{H}) \\ &\times P_s(\mathbf{s} \notin D|\mathbf{H}). \end{aligned} \tag{10}$$

Denoting the exact SD solution by $\hat{\mathbf{s}}_{\mathrm{SD}}$, it can be shown that

$$\begin{aligned} &P_s(\hat{\mathbf{s}} \neq \mathbf{s}|\mathbf{s} \in D, \mathbf{H}) \leq \\ &P_s(\hat{\mathbf{s}}_{\mathrm{SD}} \neq \mathbf{s}|\mathbf{s} \in D, \mathbf{H}) \leq \frac{P_s(\hat{\mathbf{s}}_{SD} \neq \mathbf{s}|\mathbf{H})}{P_s(\mathbf{s} \in D|\mathbf{H})}. \end{aligned} \tag{11}$$

It should be noted that the first inequality in the above equation follows from the fact that

$$P_s(\hat{\mathbf{s}}_{\mathrm{SD}} \neq \mathbf{s}|\mathbf{s} \in D, \mathbf{H}) = P_s\left(\bigcup_{\mathbf{s}_i \in e^N} \|\mathbf{y} - \mathbf{H}\mathbf{s}_i\| \leq \|\mathbf{y} - \mathbf{H}\mathbf{s}\| | \mathbf{s} \in D, \mathbf{H}\right),$$

and

$$P_s(\hat{\mathbf{s}} \neq \mathbf{s}\|\mathbf{s} \in D, \mathbf{H}) = P_s\left(\bigcup_{\mathbf{s}_i \in D} \|\mathbf{y} - \mathbf{H}\mathbf{s}_i\| \leq \|\mathbf{y} - \mathbf{H}\mathbf{s}\| | \mathbf{s} \in D, \mathbf{H}\right).$$

Therefore, since $D \subset e^N$, we have

$$P_s(\hat{\mathbf{s}} \neq \mathbf{s}|\mathbf{s} \in D, \mathbf{H}) \leq P_s(\hat{\mathbf{s}}_{\mathrm{SD}} \neq \mathbf{s}|\mathbf{s} \in D, \mathbf{H}).$$

Substituting (11) in (10), and considering the fact that $P_s(\hat{\mathbf{s}} \neq \mathbf{s}|\mathbf{s} \in D, \mathbf{H}) \leq 1$, yields

$$P_s(\hat{s} \neq \mathbf{s}|\mathbf{H}) \leq P_s(\hat{\mathbf{s}}_{\mathrm{SD}} \neq \mathbf{s}|\mathbf{H}) + P_s(\mathbf{s} \notin D|\mathbf{H}). \quad (12)$$

Theorem. *The probability of error for the proposed method for BPSK is bounded as:*

$$P_e(SD) \leq P_e \leq P_e(SD) + \kappa, \quad (13)$$

where

$$\kappa = \frac{8}{3(N_{\mathrm{r}} - N_{\mathrm{t}})!} e^{-\mathrm{th}} \left(\frac{\mathrm{SNR}^2}{4(\mathrm{th}^2 + \mathrm{SNR})}\right)^{\frac{N_{\mathrm{r}} - N_{\mathrm{t}} + 1}{2}} \times \mathcal{K}_{N_{\mathrm{r}} - N_{\mathrm{t}} + 1}\left(2\sqrt{\frac{\mathrm{th}^2 + \mathrm{SNR}}{4}}\right), \quad (14)$$

and $\mathcal{K}_\upsilon(x)$ is the modified Bessel function of the second kind defined in [30]

$$\mathcal{K}_\upsilon(x) = \int_0^\infty e^{-x\cosh t} \cosh \upsilon t dt.$$

Proof. See Appendix A.

Fortunately, the modified Bessel function is a very rapidly decreasing function of its argument as seen in Figure 9. This shows that the performance gap between the proposed method and the SD algorithm vanishes rapidly as the SNR increases.

It should be noted that the pseudo inverse computational complexity is of a polynomial order [31], while the SD search imposes an exponential computational complexity. It should also be noted that any SD algorithm must compute the QR decomposition of the channel matrix **H**. Therefore, we calculate the pseudo inverse of a triangular matrix, which has a much lower computational complexity compared to the exponential computational complexity of the SD search.

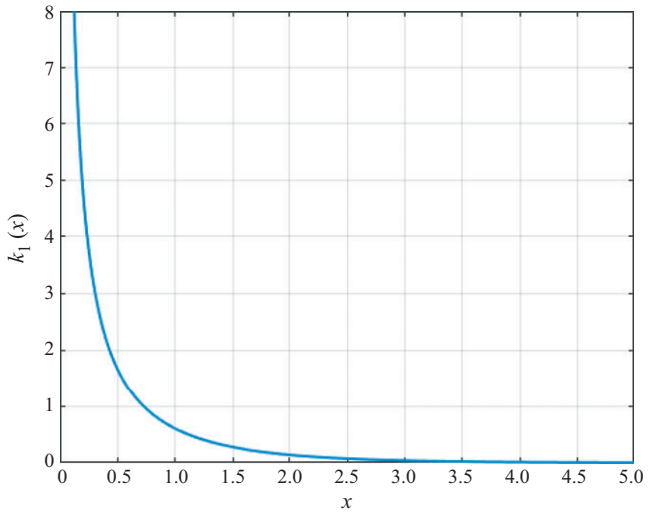

FIGURE 9 Modified Bessel function of the second kind for $v = 1$

6 | SIMULATION RESULTS

In this section, a number of numerical examples are presented. We verify the claimed theoretical results in terms of the performance and the complexity of the proposed method. All the MIMO channels are considered to be i.i.d. complex Gaussian with zero mean and unit variance. The performance of the proposed method is evaluated on the basis of symbol error rate. The number of visited nodes in the SD algorithm is also calculated in order to compare the complexity of the proposed method with that of some other detection methods. The average symbol error rate vs SNR is plotted.

6.1 | Effect of threshold on the performance of the proposed detector

In this simulation, the number of transmit and receive antennas are considered to be equal ($N_{\mathrm{r}} = N_{\mathrm{t}} = 3$), and the number of inactive antennas is considered to be $N_{\mathrm{d}} = 1$. As seen in Figure 10, as the threshold increases (th = 1, 3, 7), the error probability decreases and gets closer to the ML performance. In Figure 11, it can be seen that an increase in the threshold leads to an increase in the complexity in terms of the percentage of the total number of visited nodes. However, the complexity is always smaller

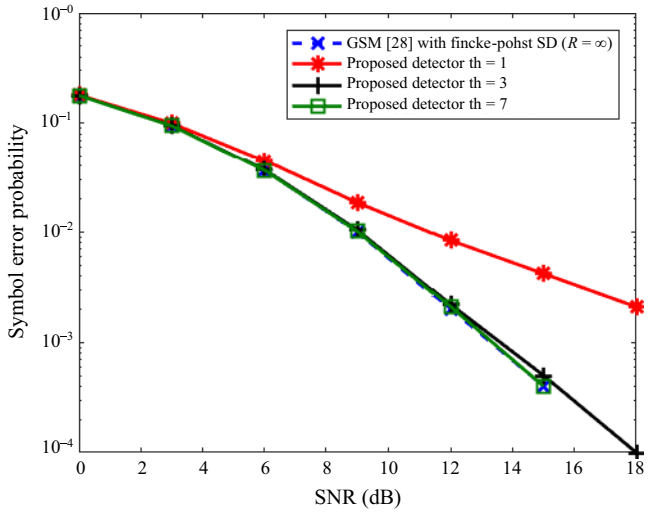

FIGURE 10 Error probability for BPSK for $N_r = N_t = 3$ and $N_d = 1$

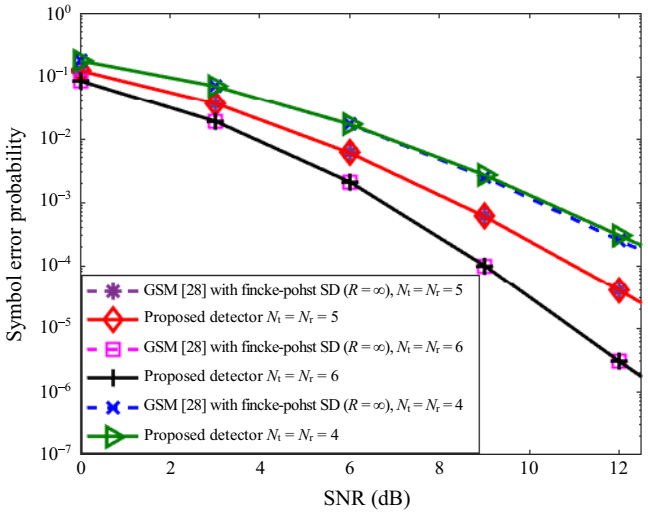

FIGURE 12 Error probability of BPSK for th = 8 and $N_d = 2$

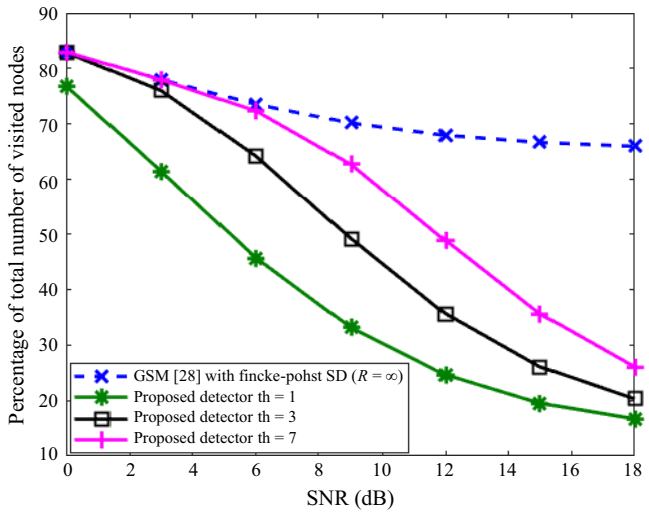

FIGURE 11 Percentage of the total number of visited nodes for BPSK for $N_r = N_t = 3$ and $N_d = 1$

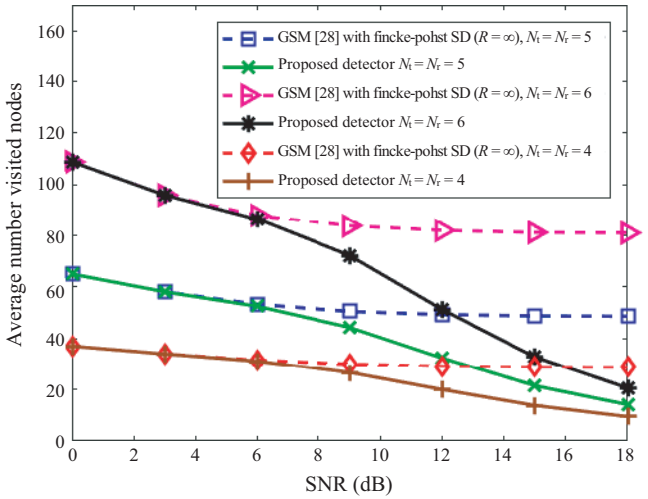

FIGURE 13 Average number of visited nodes for BPSK with th = 8 and $N_d = 2$

than that of the conventional SD method. A Fincke-Pohst SD algorithm with an initial radius $R = \infty$ combined with the GSM search strategy presented in [28] is compared with the proposed algorithm. It is worth noting that irrespective of the SD algorithm that is used, the proposed pruning algorithm reduces the number of visited nodes. According to the simulations, the proper choice of the threshold depends on the SNR and the system configurations, for example, the number of transmit and receive antennas. For instance, for a three-antenna system, it can be seen that the simulated range of SNRs (choosing th = 3) achieves a near ML performance and reduces the computational complexity considerably.

6.2 | Performance of the proposed method for different number of transmit and receive antennas

This simulation is performed with $N_d = 2$ and th = 8 for the set of transmit and receive antennas 4, 5, 6. As expected, it is seen that increasing the number of antennas increases the diversity gain, and the performance of the proposed method is equal to that of the SD method in [28] for this choice of threshold (Figure 12). In terms of complexity, this increase in the number of antennas leads to an increase in the complexity (Figure 13). Again, it can be seen that the number of visited nodes is significantly smaller than that of the sphere decoding method in [28].

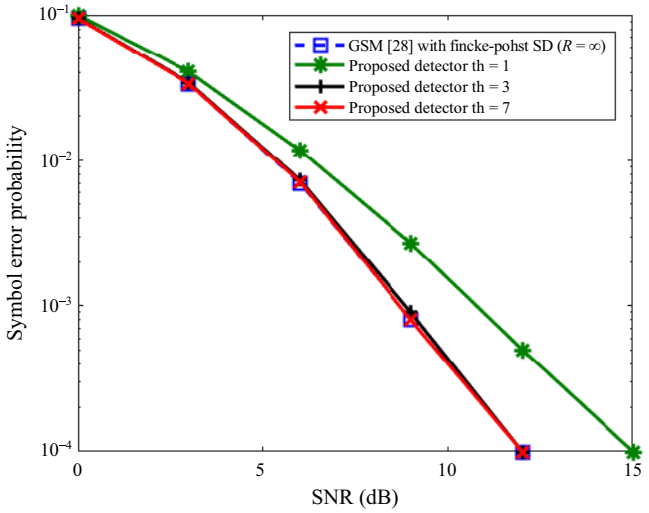

FIGURE 14 Error probability of BPSK for $N_r = 5$, $N_t = 3$, $N_d = 1$, and th = 1, 3, 7

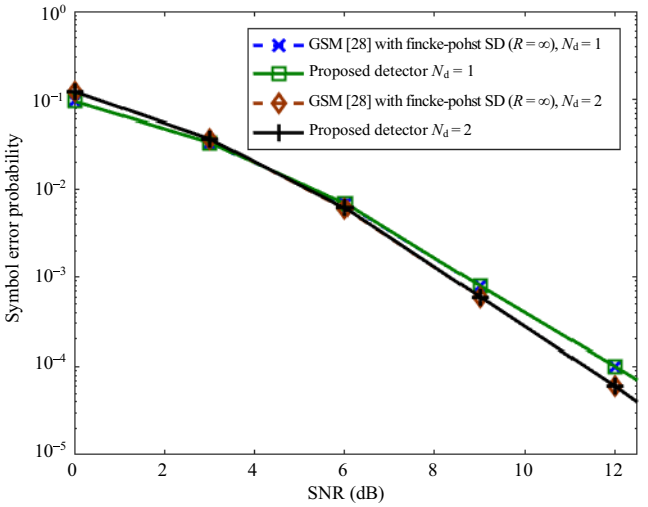

FIGURE 16 Error probability of BPSK for th = 6, and $N_r = N_t = 5$

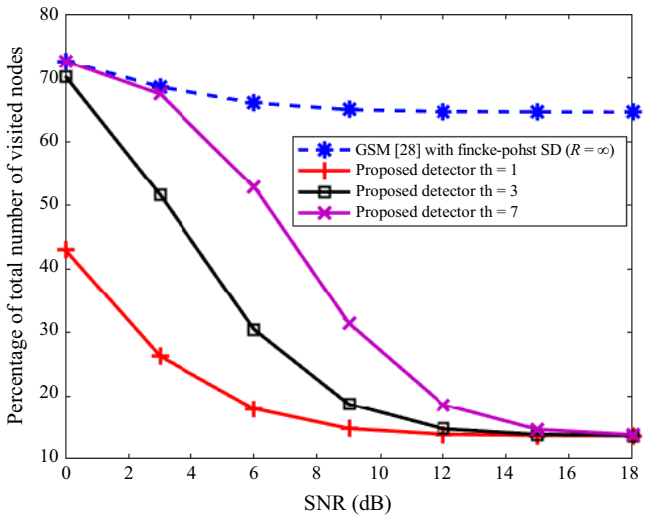

FIGURE 15 Percentage of the total number of visited nodes for BPSK with $N_r = 5$, $N_t = 3$, $N_d = 1$, and th = 1, 3, 7

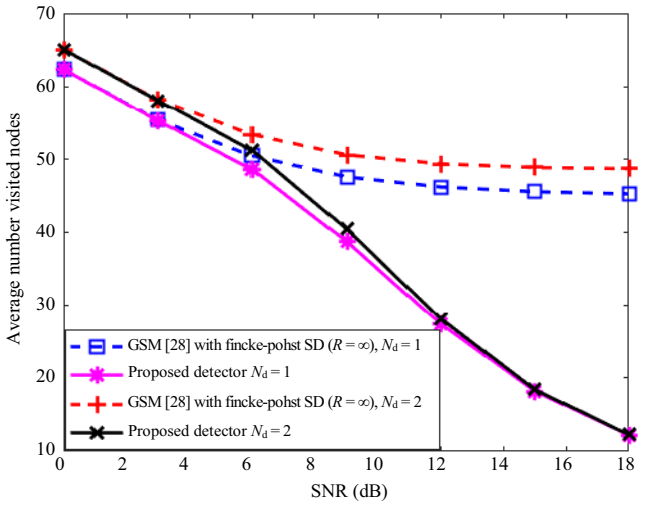

FIGURE 17 Average number of visited nodes for BPSK with th = 6, and $N_r = N_t = 5$

Figures 14 and 15 show the configuration in which the number of transmit and receive antennas are different. It can be seen that when the number of receive antennas is more than that of the transmit antennas, the ZF detected symbol is more reliable, and thus the total computational complexity is reduced.

6.3 | Effect of the number of active antennas on the performance of the proposed detector

Figures 16 and 17 show the performance of the proposed detector with $h = 6$, $N_r = N_t = 5$ for two different cases $N_d = 1$ and $N_d = 2$ Similar results can be observed in these figures.

6.4 | Theoretical performance difference between the ML and the proposed method

In this simulation, the set of assumptions th = 1, 2, and 3, and $N_r = N_t = 3$ and $N_d = 1$ are considered. Figure 18 shows that (14) decreases as the threshold increases. It also shows that the theoretical performance difference follows the simulated performance difference for almost all SNRs.

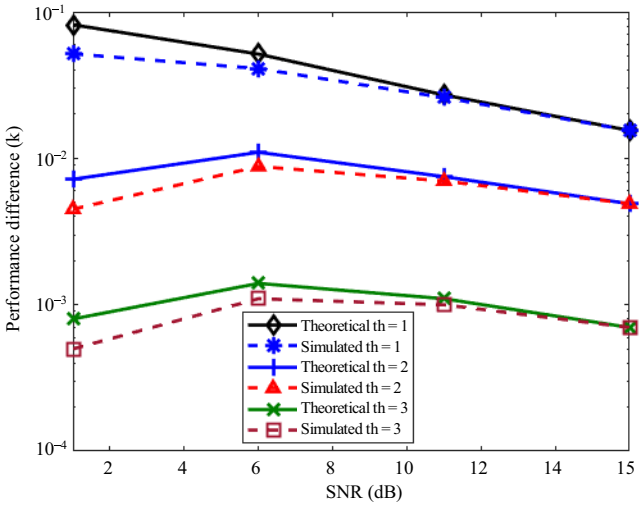

FIGURE 18 Comparison of theoretical performance difference and the simulated performance difference (14)

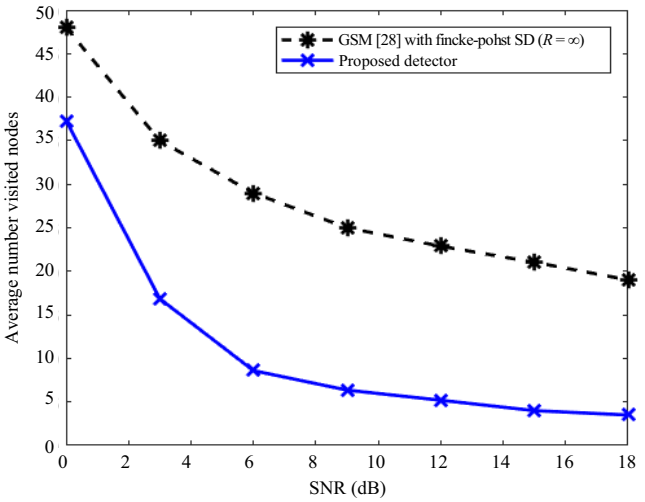

FIGURE 20 Average number of visited nodes for 16-QAM with th = 7, $N_r = N_t = 6$, and $N_d = 3$

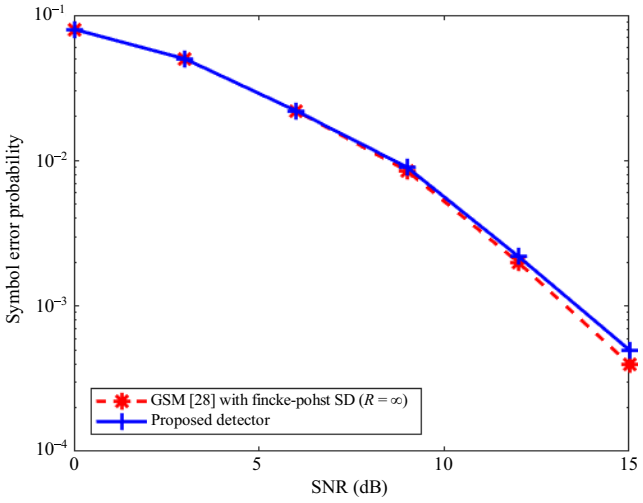

FIGURE 19 Error probability of 16-QAM for th = 7, $N_r = N_t = 6$, and $N_d = 3$

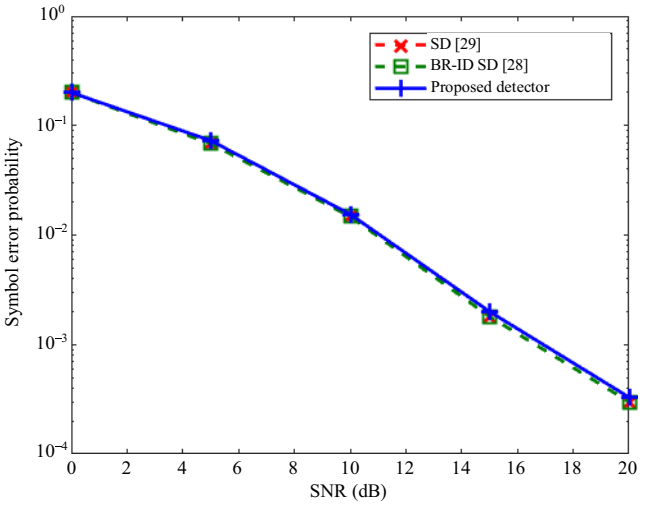

FIGURE 21 Error probability of 4QAM for th = 3, $N_r = N_t = 4$, and $N_d = 2$

6.5 | Performance of the proposed method for higher order modulations

Figures 19 and 20 show the performance and complexity of the proposed method for 16QAM modulation. In this simulation, th = 7, $N_r = N_t = 6$, and $N_d = 3$. It is observed that the proposed method achieves a near ML performance with a lower computational complexity in comparison with the method of [28].

6.6 | Application of the proposed pruning method to more powerful sphere decoders

As mentioned previously, the Fincke-Pohst SD algorithm with $R = \infty$ can be modified to reduce the number of visited nodes. Various strategies have been proposed in the literature to reduce the computational complexity of the SD algorithm. These strategies are mainly based on the introduction of an initial radius, eg [29], or a more effective body search scheme, for example, branches restriction incremental distance sphere decoding (BR-ID SD) [28]. As shown in Figures 21 and 22, we apply the proposed pruning method to the method proposed in [29], in which R is considered proportional to σ^2 and is updated if no lattice is found. The BR-ID SD method [28] and the SD method [29] are also simulated for comparison. A four-transmit-and-receive antenna system with two active antennas is considered with th = 3.

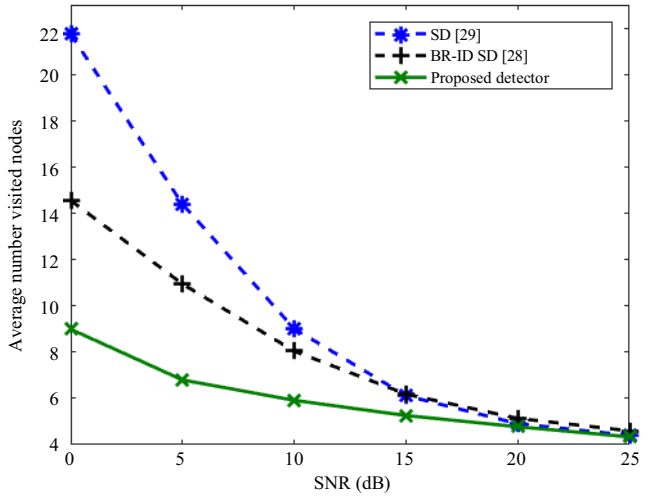

FIGURE 22 Comparison complexity of 4QAM for th = 3, $N_r = N_t = 4$, and $N_d = 2$

As seen in Figures 21 and 22, the proposed method reduces the complexity, especially at low SNRs with a near ML symbol error probability.

7 | CONCLUSION

In this paper, we proposed a ZF-based detector combined with the SD method to reduce the computational complexity while achieving a near ML performance. We analyzed the performance of the proposed method and provided an analysis of the performance difference between the proposed method and the ML detector. Simulation results showed that the performance of the proposed method is very close to that of the ML detector while achieving a significant computational complexity reduction compared to the conventional SD method in terms of the number of visited nodes. We provided an analytic performance gap between the proposed detector and the ML detector. We also presented some simulations to assess the accuracy of our theoretical results.

ORCID

Majid Fouladian https://orcid.org/0000-0002-3865-6190

REFERENCES

1. L. Zheng and D. N. C. Tse, *Diversity and multiplexing: a fundamental tradeoff in multiple-antenna channels*, IEEE Trans. Inform. Theory **49** (2013), no. 5, 1073–1096.
2. D. Tse and P. Viswanath, *Fundamentals of wireless communications*, Cambridge University Press, Cambridge, UK, 2005.
3. G. T. Foschini and M. J. Gans, *On limits of wireless communication in a fading environment when using multiple antennas*, Wireless Pers. Commun. **6** (1998), no. 3, 311–335.
4. E. Telatar, *Capacity of multi-antenna Gaussian channels*, Eur. Trans. Telecommun. **10** (1999), no. 6, 585–596.
5. A. Paularj, *An introduction to space-time wireless communication systems*, Cambridge University Press, Cambridge, UK, 2003.
6. R. Meseleh et al., Spatial modulation a new low Complexity spectral efficiency enhancing technique, In *Int. Conf. Commun. Netw.*, China, Oct. 25–27, 2006, pp. 1–5.
7. A. Younis et al., Generalised spatial modulation, In *Proc. Asilomar Conf. Signals, Syst. Comput.*, Pacific Grove, CA, USA, Nov. 7–10, 2010, pp. 1498–1502.
8. J. Fu et al., Generalised spatial modulation with multiple active transmit antennas, In *Proc. IEEE GLOBECOM*, Miami, FL, USA, Dec. 8–10, 2010, pp. 839–844.
9. U. Fincke and M. Pohst, *Improved methods for calculating vectors of short length in a lattice, including a complexity analysis*, Math. Comput. **44** (1985), no. 170, 463–471.
10. H. Vikalo and B. Hassibi, *On the sphere-decoding algorithm. II. Generalization, second-order statistics, and applications to communications*, IEEE Trans. Signal Process. **53** (2005), no. 8, 2819–2834.
11. L. G. Barbero and J. S. Thompson, *Fixing the complexity of the sphere decoder or MIMO detection*, IEEE Trans. Wireless Commun. **7** (2008), no. 6, 2131–2142.
12. J. W. Choi et al., *Low-complexity decoding via reduced dimension maximum-likelihood search*, IEEE Trans. Signal Process. **58** (2010), no. 3, 1780–1793.
13. J. Jalden et al., *The error probability of the fixed-complexity sphere decoder*, IEEE Trans. Signal Process. **57** (2009), no. 7, 2711–2720.
14. R. H. Chen and W. H. Chung, *Reduced complexity MIMO detection scheme using statistical search space reduction*, IEEE Commun. Lett. **16** (2012), no. 3, 292–295.
15. B. Shim and I. Kang, *Sphere decoding with a probabilistic tree pruning*, IEEE Trans. Signal Process. **56** (2008), no. 10, 4867–4878.
16. M. Neinavaie and M. Derakhtian, *ML performance achieving algorithm with the zero-forcing complexity at high SNR regime*, IEEE Trans. Wireless Commun. **15** (2016), no. 7, 4651–4659.
17. Y. Jiang et al., *Performance analysis of ZF and MMSE equalizers for MIMO systems: a in-depth study of the high SNR regime*, IEEE Trans. Inform. Theory **57** (2011), no. 4, 2008–2026.
18. A. K. Lenstra et al., *Factoring polynomials with rational coefficient*, Math. Annu. **261** (1982), no. 4, 515–534.
19. M. Taherzadeh, A. Mobasher, and A. K. Khandani, *LLL reduction achieves the receive diversity in MIMO decoding*, IEEE Trans. Inform. Theory **53** (2007), no. 12, 4801–4805.
20. M. Di Renzo et al., *Spatial modulation for generalized MIMO: challenges, opportunities, and implementation*, Proc. IEEE **102** (2014), no. 1, 56–103.
21. P. Yang et al., *Design guidelines for spatial modulation*, IEEE Commun. Surveys Tutorials **17** (2015), no. 1, 6–26.
22. G. H. Lee and T. H. Kim, *Implementation of a near-optimal detector for spatial modulation MIMO systems*, IEEE Trans. Circuits Syst. II, **63** (2016), no. 10, 954–958.
23. Y. Xiao et al., *Low-complexity signal detection for generalized spatial modulation*, IEEE Commun. Lett. **18** (2014), no. 3, 403–406.

24. C. E. Chen, C. H. Li, and Y. H. Huang, *An improved ordered-block MMSE detector for generalized spatial modulation*, IEEE Commun. Lett. **19** (2015), no. 5, 707–710.
25. A. Younis et al., *Generalised sphere decoding for spatial modulation*, IEEE Trans. Commun. **61** (2013), no. 7, 2805–2815.
26. A. Younis et al., Sphere decoding for spatial modulation, In *Proc. Intell. Conf. Commun. IEEE*, Kyoto, Japan, June 5–9, 2011, pp. 1–6.
27. A. Younis et al., Reduced complexity sphere decoder for spatial modulation detection receivers, In *Proc. Global Telecommun. Conf. IEEE*, Miami, FL, USA, Dec. 6–10, 2010, pp. 1–5.
28. J. A. Cal-Braz and R. Sampaio-Neto, *Low-complexity sphere decoding detector for generalized spatial modulation systems*, IEEE Commun. Lett. **18** (2014), no. 6, 949–952.
29. B. Hassibi and H. Vikalo, *On the sphere decoding algorithm I. Expected complexity*, IEEE Trans. Signal Process. **53** (2005), no. 8, 2806–2818.
30. M. Abramowitz and I. A. Stegun, *Handbook of mathematical functions with formulas, graphs, and mathematical tables*, U.S. Department of Commerce, Boulder, CO, USA, 1972.
31. C. Tang et al., *High precision low complexity matrix inversion based on Newton iteration for data detection in the massive MIMO*, IEEE Commun. Lett. **20** (2016), no. 3, 490–493.
32. I. S. Gradshteyn and I. M. Ryzhik, *Table of integrals, series and products*, Academic, New York, NY, USA, 1980.

AUTHOR BIOGRAPHIES

Sara Jafarpoor received her BSc degree in electrical engineering from the Islamic Azad University of Fasa, Iran, in 2007, and her MSc degree in communication systems from the Islamic Azad University of Bushehr, Iran, in 2012. At present, she is a PhD student at the Department of Electrical Engineering, College of Technical and Engineering Saveh Branch, Islamic Azad University, Iran. Her current research interests include wireless communications, mobile networks, detection theory, and MIMO communication systems.

Majid Fouladian received his MS degree in communication systems from the Isfahan University of Technology, Isfahan, Iran in 2008, and PhD degree in communication systems from the Islamic Azad University Science and Research Branch, Tehran, Iran in 2016. He is currently a faculty member at the Department of Electrical Engineering, College of Technical and Engineering, Saveh Branch, Islamic Azad University, Iran. His current research interests include mobile networks, next generation wireless systems, and vehicular communication systems, with a focus on routing and medium access control protocols, resource management, and analysis of network architectures and protocols.

Mohammad Neinavaie was born in Shiraz, Iran, in 1983. He received his MSc and PhD degrees in communication systems engineering from the University of Shiraz, Iran, in 2009 and 2015, respectively. His research interests include detection theory, information theory, wireless communications, statistical signal processing, MIMO communication systems, and co-operative communications.

APPENDIX A

PROOF OF THEOREM

We assume that the kth transmitted symbol is c_i, that is, $s_k = c_i$. Using the union bound, ie $\bigcup_{i=1}^{N} A_i \leq \sum_{i=1}^{N} P(A_i)$, results in

$$P(s_k \notin D_k) = P\left(\bigcup_{k=1}^{N_t} s_k \notin D_k\right) \leq \sum_{K=1}^{N_t} (s_k \notin D_k), \quad \text{(A1)}$$

where D_k is the search space.

One can expand $P(s_k \notin D_k)$ depending on the event that the transmitted symbol is one of the zero or not zero constellation points, as:

$$\begin{aligned} P(s_k \notin D_k) &= E_{\mathbf{H}}\{P(s_k \notin D_k | s_k = 0, \mathbf{H})P(s_k = 0) \\ &+ P(s_k \notin D_k | s_k = 1, \mathbf{H})P(s_k = 1) \\ &+ P(s_k \notin D_k | s_k = -1, \mathbf{H})P(s_k = -1)\}. \end{aligned} \quad \text{(A2)}$$

In order to simplify (A2), we need to calculate the terms $P(s_k \notin D_k | s_k = 0, \mathbf{H})$, $P(s_k \notin D_k | s_k = 1, \mathbf{H})$, and $P(s_k \notin D_k | s_k = -1, \mathbf{H})$.

Assuming $s_k = 0$, the event $s_k \notin D_k$ happens when $\tilde{y}_k \in \overline{\mathrm{ZR}}$ or when $\mathcal{E}_1$ occurs. The set $\overline{\mathrm{ZR}}$ is complementary to the set ZR. Therefore,

$$P(s_k \notin D_k | s_k = 0, \mathbf{H}) = P\left(\tilde{y} \in \overline{\mathrm{ZR}} \cup (\mathcal{E}_1)\right), \quad \text{(A3)}$$

where the event $\mathcal{E}_1$ is the event that $\tilde{y}_m \in \mathrm{ZR}, \tilde{y}_m < \tilde{y}_k$, $s_m \neq 0$ for $m \neq k$.

The probability of $\mathcal{E}_1$ can be expressed as:

$$\begin{aligned} P(\mathcal{E}_1) &\le P(\tilde{y}_m \in \mathrm{ZR}, \mathrm{s}_m \neq 0) \\ &= P\left(\tilde{y}_{m\in\ \mathrm{ZR}|\mathrm{s}_m\neq 0}\right) P(s_m \neq 0). \end{aligned} \tag{A4}$$

Therefore, we have

$$\begin{aligned} P(s_k \notin D_k | s_k = 0, \mathbf{H}) &\le P\left(\tilde{y}_k \in \overline{\mathrm{ZR}}\right) \\ &+ P(\tilde{y}_m \in \mathrm{ZR} | s_m \neq 0) P(s_m \neq 0). \end{aligned} \tag{A5}$$

Given $s_k = 0$ and H, the pdf of $\tilde{y}_k$ can be written as:

$$f(\tilde{y}_k | \{s_k = 0, \mathbf{H}) = \frac{1}{\sqrt{2\pi\sigma_k^2}} \exp\left(-\frac{\tilde{y}_k^2}{2\sigma_k^2}\right) d_{\tilde{y}_k} \tag{A6}$$

Thus, we can write

$$\begin{aligned} &P(\tilde{y}_k \in \overline{\mathrm{ZR}} | s_k = 0, \mathbf{H}) \\ &= \int_{-\infty}^{\frac{-1}{2} - \mathrm{th}_k} \frac{1}{\sqrt{2\pi\sigma_k^2}} \exp\left(\frac{-\tilde{y}_k^2}{2\sigma_{\mathrm{k}}^2}\right) d_{\tilde{y}_k} \\ &+ \int_{\frac{1}{2}+\mathrm{th}_k}^{\infty} \frac{1}{\sqrt{2\pi\sigma_k^2}} \exp\left(\frac{-\tilde{y}_k^2}{2\sigma_k^2}\right) d_{\tilde{y}_k}. \end{aligned} \tag{A7}$$

According to the definition of the function Q, ie:

$$\mathrm{Q}(x) = \int_x^{\infty} \frac{1}{\sqrt{2\pi}} \exp\left(\frac{-x^2}{2}\right) d_x, \tag{A8}$$

and by defining the variable $\tilde{z}_k = \frac{\tilde{y}_k}{\sigma_k}$, we can rewrite (A7) as:

$$\begin{aligned} &P(\tilde{y}_k \in \overline{\mathrm{ZR}} | s_k = 0, \mathbf{H}) \\ &= \int_{-\infty}^{\frac{\frac{-1}{2} - \mathrm{th}_k}{\sigma_k}} \frac{1}{\sqrt{2\pi}} \exp\left(\frac{-\tilde{z}_k^2}{2}\right) d_{\tilde{z}_k} \\ &+ \int_{\frac{\frac{1}{2}+\mathrm{th}_k}{\sigma_k}}^{\infty} \frac{1}{\sqrt{2\pi}} \exp\left(\frac{-\tilde{\mathrm{z}}_k^2}{2}\right) d_{\tilde{z}_k} = 2Q\left(\mathrm{th}\sigma_k + \frac{1}{2\sigma_k}\right), \end{aligned} \tag{A9}$$

where $\sigma_k = \sqrt{\sigma^2 [(\mathbf{H}^{\mathrm{H}}\mathbf{H})^{-1}]_{kk}}$, $[(\mathbf{H}^{\mathrm{H}}\mathbf{H})^{-1}]_{kk} = \tau_k$ and $\mathrm{SNR} = \frac{1}{\sigma^2}$. Hence, we have

$$P(\tilde{\mathrm{y}}_k \in \overline{\mathrm{ZR}} | s_k = 0, \mathbf{H}) = 2Q\left(\mathrm{th}\sqrt{\frac{\tau_k}{\mathrm{SNR}}} + \frac{1}{2}\sqrt{\frac{\mathrm{SNR}}{\tau_k}}\right). \tag{A10}$$

Now, given $s_m = 1$, the pdf of $\tilde{y}_m$ is

$$f(\tilde{y}_m | s_m = 1, \mathbf{H}) = \frac{1}{\sqrt{2\pi\sigma_m^2}} \exp\left(\frac{-(\tilde{y}_m - 1)^2}{2\sigma_m^2}\right), \tag{A11}$$

and consequently,

$$\begin{aligned} &P(\tilde{y}_m \in \overline{\mathrm{ZR}} | s_m = 1, \mathbf{H}) \\ &= \int_{\frac{1}{2}+\mathrm{th}_m}^{\frac{1}{2}-\mathrm{th}_m} \frac{1}{\sqrt{2\pi\sigma_x^2}} \exp\left(\frac{-(\tilde{y}_m - 1)^2}{2\sigma_m^2}\right) \mathrm{d}_{\tilde{y}_m} \\ &= 1 - \int_{-\infty}^{\frac{-1}{2}+\mathrm{th}_m} \frac{1}{\sqrt{2\pi\sigma_m^2}} \exp\left(\frac{-(\tilde{y}_m - 1)^2}{2\sigma_m^2}\right) d_{\tilde{y}_m} \\ &- \int_{\frac{1}{2}-\mathrm{th}_m}^{\infty} \frac{1}{\sqrt{2\pi\sigma_m^2}} \exp\left(\frac{-(\tilde{y}_m - 1)^2}{2\sigma_m^2}\right) \mathrm{d}_{\tilde{y}_m}. \end{aligned} \tag{A12}$$

According to the definition of the function Q and by defining the variable $\tilde{z}_m = \frac{\tilde{y}_m - 1}{\sigma_m}$, we can write:

$$\begin{aligned} &P(\tilde{y}_m \in \overline{\mathrm{ZR}} | s_m = 1, \mathbf{H}) \\ &= 1 - \int_{-\infty}^{\frac{\frac{-3}{2}+\mathrm{th}_m}{\sigma_m}} \frac{1}{\sqrt{2\pi}} \exp\left(\frac{-\tilde{z}_m^2}{2}\right) d_{\tilde{\mathrm{z}}_m} \\ &- \int_{\frac{\frac{-1}{2}+\mathrm{th}_m}{\sigma_m}}^{\infty} \frac{1}{\sqrt{2\pi}} \exp\left(\frac{-\tilde{z}_m^2}{2}\right) d_{\tilde{\mathrm{z}}_m} \\ &= Q\left(\mathrm{th}\sigma_m + \frac{1}{2\sigma_m}\right) - Q\left(\frac{3}{2\sigma_m} - \mathrm{th}\sigma_m\right), \end{aligned} \tag{A13}$$

where $\sigma_m = \sqrt{\sigma^2 [(\mathbf{H}^{\mathrm{H}}\mathbf{H})^{-1}]_{mm}}$, $[(\mathbf{H}^{\mathrm{H}}\mathbf{H})^{-1}]_{mm} = \tau_m$ and $\mathrm{SNR} = \frac{1}{\sigma^2}$.
Hence,

$$\begin{aligned} P(\tilde{y}_m \in \overline{\mathrm{ZR}} | s_m = 1, \mathbf{H}) &= Q\left(\mathrm{th}\sqrt{\frac{\tau_m}{\mathrm{SNR}}} + \frac{1}{2}\sqrt{\frac{\mathrm{SNR}}{\tau_m}}\right) \\ &- Q\left(\frac{3}{2}\sqrt{\frac{\mathrm{SNR}}{\tau_m}} - \mathrm{th}\sqrt{\frac{\tau_m}{\mathrm{SNR}}}\right). \end{aligned} \tag{A14}$$

The same calculations can be applied for $P(\tilde{y}_m \in \mathrm{ZR} | s_m = -1, \mathbf{H})$. Thus, we have

$$\begin{aligned} P(s_k \notin D_k | s_k = 0, \mathbf{H}) &\le 2Q\left(\mathrm{th}\sqrt{\frac{\tau_k}{\mathrm{SNR}}} + \frac{1}{2}\sqrt{\frac{\mathrm{SNR}}{\tau_k}}\right) \\ &+ \frac{4}{3}Q\left(\mathrm{th}\sqrt{\frac{\tau_m}{\mathrm{SNR}}} + \frac{1}{2}\sqrt{\frac{\mathrm{SNR}}{\tau_m}}\right) \\ &- \frac{4}{3}Q\left(\frac{3}{2}\sqrt{\frac{\mathrm{SNR}}{\tau_m}} - \mathrm{th}\sqrt{\frac{\tau_m}{\mathrm{SNR}}}\right). \end{aligned} \tag{A15}$$

Now, we consider $P(s_k \notin D_k | s_k = 0, \mathbf{H})$. Assuming $s_k \neq 0$, we have

$$P(s_k \notin D_k | s_k = 1, \mathbf{H}) = P(\tilde{y}_k \in \overline{\mathrm{R1}} \cup (\mathcal{E}_2)), \tag{A16}$$

and

$$P(s_k \notin D_k | s_k = 1, \mathbf{H}) = P(\tilde{y}_k \in \overline{\mathrm{R}-1} \cup (\mathcal{E}_2)), \tag{A17}$$

where the event $\mathcal{E}_2$ is the event that $\tilde{y}_m \in \overline{\mathrm{ZR}}$, $\tilde{y}_m > \tilde{y}_k$, $s_m = 0$ for $m \neq k$.

The probability of $\mathcal{E}_1$ can be expressed as:

$$\begin{aligned} P(\mathcal{E}_2) &\leq P(\tilde{y}_m \in \overline{\mathrm{ZR}}, s_m = 0) \\ &= P(\tilde{y}_m \in \overline{\mathrm{ZR}} | s_m = 0) P(s_m = 0). \end{aligned} \tag{A18}$$

We have,

$$\begin{aligned} P(s_k \notin D_k | s_k = 1, \mathbf{H}) &\leq P(\tilde{y}_k \in \overline{\mathrm{R1}}) \\ &+ P(\tilde{y}_m \in \overline{\mathrm{ZR}} | s_m = 0) P(s_m = 0), \end{aligned} \tag{A19}$$

where the pdf of $\tilde{y}_k$ can be written as:

$$f(\tilde{y}_k | s_k = 1, \mathbf{H}) = \frac{1}{\sqrt{2\pi\sigma_k^2}} \exp\left(\frac{-(\tilde{y}_k - 1)^2}{2\sigma_k^2} \right) d_{\tilde{y}_k}. \tag{A20}$$

Thus,

$$P(\tilde{y}_k \in \overline{\mathrm{R1}} | s_k = 1, \mathbf{H}) = \int_{-\infty}^{\frac{1}{2} - \mathrm{th}_k} \frac{1}{\sqrt{2\pi\sigma_k^2}} \exp\left(\frac{-(\tilde{y}_k - 1)^2}{2\sigma_k^2} \right) d_{\tilde{y}_k}. \tag{A21}$$

According to the definition of the function Q and by defining the variable $\tilde{z}_k = \frac{\tilde{y}_k - 1}{\sigma_k}$, we can write:

$$\begin{aligned} &P(\tilde{y}_k \in \overline{\mathrm{R1}} | s_k = 1, \mathbf{H}) \\ &= \int_{-\infty}^{-\left(\frac{\mathrm{th}_k + \frac{1}{2}}{\sigma_k} \right)} \frac{1}{\sqrt{2\pi}} \exp\left(-\frac{(\tilde{z}_k)^2}{2} \right) d_{\tilde{z}_k} \\ &= Q\left(\mathrm{th}\sigma_k + \frac{1}{2\sigma_k} \right). \end{aligned} \tag{A22}$$

Similarly, we have

$$P(\tilde{y}_k \in \overline{\mathrm{R1}} | s_k = 1, \mathbf{H}) = Q\left(\mathrm{th}\sqrt{\frac{\tau_k}{\mathrm{SNR}}} + \frac{1}{2}\sqrt{\frac{\mathrm{SNR}}{\tau_k}} \right), \tag{A23}$$

and for $P(\tilde{y}_m \in \overline{\mathrm{ZR}} | s_m = 0, \mathbf{H})$, we can write

$$P(\tilde{y}_m \in \overline{\mathrm{ZR}} | s_m = 0, \mathbf{H}) = 2Q\left(\mathrm{th}\sqrt{\frac{\tau_m}{\mathrm{SNR}}} + \frac{1}{2}\sqrt{\frac{\mathrm{SNR}}{\tau_m}} \right). \tag{A24}$$

Therefore,

$$\begin{aligned} P(s_k \notin D_k | s_k = 1, \mathbf{H}) &\leq Q\left(\mathrm{th}\sqrt{\frac{\tau_k}{\mathrm{SNR}}} + \frac{1}{2}\sqrt{\frac{\mathrm{SNR}}{\tau_k}} \right) \\ &+ \frac{4}{3} Q\left(\mathrm{th}\sqrt{\frac{\tau_m}{\mathrm{SNR}}} + \frac{1}{2}\sqrt{\frac{\mathrm{SNR}}{\tau_m}} \right). \end{aligned} \tag{A25}$$

Now, for $P(s_k \notin D_k | s_k = -1, \mathbf{H})$, we have

$$\begin{aligned} P(\mathrm{s}_k \notin D_k | s_k = -1, \mathbf{H}) &\leq \mathrm{P}(\tilde{\mathrm{y}}_k \in \overline{\mathrm{R}-1}) \\ &+ P(\tilde{y}_m \in \overline{\mathrm{ZR}} | s_m = 0) P(s_m = 0). \end{aligned} \tag{A26}$$

Given $s_k = -1$, the pdf of $\tilde{y}_k$ can be expressed as:

$$f(\tilde{y}_k | s_k = -1, \mathbf{H}) = \frac{1}{\sqrt{2\pi\sigma_k^2}} \exp\left(-\frac{(\tilde{y}_k - 1)^2}{\sigma_k^2} \right) d_{\tilde{y}_k}. \tag{A27}$$

Thus, we have

$$\begin{aligned} &P(\tilde{y}_k \in \overline{\mathrm{R}-1} | s_k = -1, \mathbf{H}) \\ &= \int_{\frac{1}{2} + th_k}^{\infty} \frac{1}{\sqrt{2\pi\sigma_k^2}} \exp\left(-\frac{(\tilde{y}_k + 1)^2}{2\sigma_k^2} \right) d_{\tilde{y}_k}. \end{aligned} \tag{A28}$$

As with (A22), we can write:

$$\begin{aligned} P(\tilde{y}_k \in \overline{\mathrm{R}-1} | s_k = -1, \mathbf{H}) &= \int_{\frac{\frac{1}{2} + th_k}{\sigma_k}}^{\infty} \frac{1}{\sqrt{2\pi}} \exp\left(-\frac{\tilde{z}_k^2}{2} \right) d_{\tilde{z}_k} \\ &= \mathrm{Q}\left(\mathrm{th}\sqrt{\frac{\tau_k}{\mathrm{SNR}}} + \frac{1}{2}\sqrt{\frac{\mathrm{SNR}}{\tau_k}} \right). \end{aligned} \tag{A29}$$

Therefore,

$$\begin{aligned} P(\tilde{y}_k | s_k = -1, \mathbf{H}) &\leq \mathrm{Q}\left(\mathrm{th}\sqrt{\frac{\tau_k}{\mathrm{SNR}}} + \frac{1}{2}\sqrt{\frac{\mathrm{SNR}}{\tau_k}} \right) \\ &+ \frac{4}{3} \mathrm{Q}\left(\mathrm{th}\sqrt{\frac{\tau_m}{\mathrm{SNR}}} + \frac{1}{2}\sqrt{\frac{\mathrm{SNR}}{\tau_m}} \right). \end{aligned} \tag{A30}$$

Finally, we can express (A2) as:

$$\begin{aligned} P(s_k \notin D_k) &\leq E_{\mathbf{H}} \Bigg\{ \frac{1}{3} \Bigg(\mathrm{Q}\left(\mathrm{th}\sqrt{\frac{\tau_k}{\mathrm{SNR}}} + \frac{1}{2}\sqrt{\frac{\mathrm{SNR}}{\tau_k}} \right) + \\ &2\mathrm{Q}\left(\mathrm{th}\sqrt{\frac{\tau_k}{\mathrm{SNR}}} + \frac{1}{2}\sqrt{\frac{\mathrm{SNR}}{\tau_k}} \right) \\ &+ \mathrm{Q}\left(\mathrm{th}\sqrt{\frac{\tau_k}{\mathrm{SNR}}} + \frac{1}{2}\sqrt{\frac{\mathrm{SNR}}{\tau_k}} \right) \Bigg) \\ &+ \frac{2}{3} \Bigg(2\mathrm{Q}\left(\mathrm{th}\sqrt{\frac{\tau_m}{\mathrm{SNR}}} + \frac{1}{2}\sqrt{\frac{\mathrm{SNR}}{\tau_m}} \right) \\ &+ 2\mathrm{Q}\left(\mathrm{th}\sqrt{\frac{\tau_m}{\mathrm{SNR}}} + \frac{1}{2}\sqrt{\frac{\mathrm{SNR}}{\tau_m}} \right) \\ &- 2\mathrm{Q}\left(\frac{3}{2}\sqrt{\frac{\mathrm{SNR}}{\tau_m}} - \mathrm{th}\sqrt{\frac{\tau_m}{\mathrm{SNR}}} \right) \\ &+ 2\mathrm{Q}\left(\mathrm{th}\sqrt{\frac{\tau_m}{\mathrm{SNR}}} + \frac{1}{2}\sqrt{\frac{\mathrm{SNR}}{\tau_m}} \right) \Bigg) \Bigg\} \\ &\leq E_{\mathrm{H}} \Bigg\{ \frac{1}{3} \Bigg(\Bigg(4Q\left(\mathrm{th}\sqrt{\frac{\tau_k}{\mathrm{SNR}}} + \frac{1}{2}\sqrt{\frac{\mathrm{SNR}}{\tau_k}} \right) \Bigg) \\ &+ \frac{2}{3} \Bigg(6\mathrm{Q}\left(\mathrm{th}\sqrt{\frac{\tau_m}{\mathrm{SNR}}} + \frac{1}{2}\sqrt{\frac{\mathrm{SNR}}{\tau_m}} \right) \Bigg) \Bigg) \Bigg\}. \end{aligned} \tag{A31}$$

Using the equality $Q(x) < \frac{1}{2} e^{\frac{-x^2}{2}}$ for the function Q, we have

$$E_{\tau_{km}}\left\{\mathrm{Q}\left(\mathrm{th}\sqrt{\frac{\tau_k}{\mathrm{SNR}}}+\frac{1}{2}\sqrt{\frac{\mathrm{SNR}}{\tau_k}}\right)\right\}$$
$$\leq \int_0^{\infty}\frac{1}{2}\exp\left(-\left(\mathrm{th}\sqrt{\frac{\tau_k}{\mathrm{SNR}}}+\frac{1}{2}\sqrt{\frac{\mathrm{SNR}}{\tau_k}}\right)^2\right), \quad \text{(A32)}$$
$$\times\frac{1}{(N_\mathrm{r}-N_\mathrm{t})!}\tau_k^{N_\mathrm{r}-N_\mathrm{t}}e^{-\tau_k}\mathrm{d}\tau_k$$

which can be simplified as:

$$\frac{1}{(N_\mathrm{r}-N_\mathrm{t})!}\times\frac{8}{6}e^{-\mathrm{th}}\int_0^{\infty}e^{-\left(\frac{\mathrm{th}^2}{\mathrm{SNR}}+1\right)\tau_k}e^{\frac{-\mathrm{SNR}}{4\tau_k}}\tau_k^{\frac{N_\mathrm{r}-N_\mathrm{t}}{1}}\mathrm{d}\tau_k. \quad \text{(A33)}$$

Now, according to the integral [32]:

$$\int_0^{\infty}\mathrm{y}^{v-1}\mathrm{e}^{\frac{-\beta}{y}}\mathrm{e}^{-\gamma y}dy=2\left(\frac{\beta}{\gamma}\right)^{\frac{v}{2}}\mathcal{K}_v(2\sqrt{\beta\gamma}), \quad \text{(A34)}$$

where $\mathcal{K}_v(x)$ is the modified Bessel function of the second kind [30]. For $v-1=N_\mathrm{r}-N_\mathrm{t}$, $\gamma=\frac{\mathrm{th}^2}{\mathrm{SNR}}+1=\frac{\mathrm{th}^2+\mathrm{SNR}}{\mathrm{SNR}}$ and $\beta=\frac{\mathrm{SNR}}{4}$, we have

$$\frac{1}{(N_\mathrm{r}-N_\mathrm{t})!}\times\frac{8}{6}e^{-\mathrm{th}}\int_0^{\infty}e^{\left(-\frac{\mathrm{th}^2}{\mathrm{SNR}}+1\right)\tau_k}e^{\frac{-\mathrm{SNR}}{4\tau_k}}\tau_k^{\frac{N_\mathrm{r}-N_\mathrm{t}}{1}}d\tau_k$$
$$=\frac{8}{3(N_\mathrm{r}-N_\mathrm{t})!}e^{-\mathrm{th}}\left(\frac{\mathrm{SNR}^2}{4(\mathrm{th}^2+\mathrm{SNR})}\right)^{\frac{N_\mathrm{r}-N_\mathrm{t}+1}{2}}$$
$$\times\mathcal{K}_{N_\mathrm{r}-N_\mathrm{t}+1}\left(2\sqrt{\frac{\mathrm{th}^2+\mathrm{SNR}}{4}}\right). \quad \text{(A35)}$$

Finally, we rewrite the error probability in equality as (13) and (14).